IEEE Photonics Journal
An IEEE Photonics Society Publication

Multiple Competition Processes Between Stimulated Brillouin and Raman Scattering in a Sulfate Aqueous Solution

Volume 9, Number 2, April 2017

Jiulin Shi
Zuhao Yang
Chenpeng Cao
Yubao Zhang
Shengpeng Wan
Xingdao He
Zhongping Chen

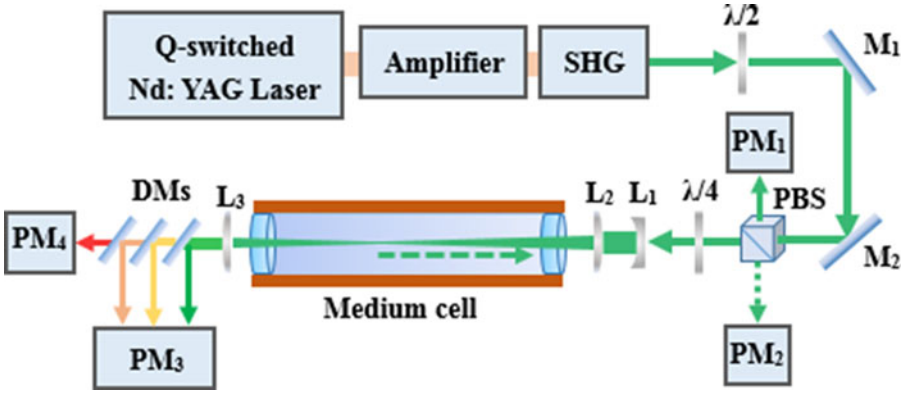

DOI: 10.1109/JPHOT.2017.2689072
1943-0655

Multiple Competition Processes Between Stimulated Brillouin and Raman Scattering in a Sulfate Aqueous Solution

Jiulin Shi, Zuhao Yang, Chenpeng Cao, Yubao Zhang, Shengpeng Wan, Xingdao He, and Zhongping Chen

Jiangxi Engineering Laboratory for Optoelectronics Testing Technology and National Engineering Laboratory for Nondestructive Testing and Optoelectric Sensing Technology and Application, Nanchang Hangkong University, Nanchang 330063, China

DOI:10.1109/JPHOT.2017.2689072

Manuscript received February 7, 2017; revised March 20, 2017; accepted March 26, 2017. Date of publication March 29, 2017; date of current version April 11, 2017. This work was supported in part by the National Natural Science Foundation of China under Grant 41666004, Grant 41576033, and Grant 61465009; in part by the Project of the Education Department of Jiangxi Province under Grant GJJ150728; and in part by the Graduate Student Innovation Foundation of Jiangxi Province under Grant YC2016-S338 and Grant YC2016055. Corresponding authors: J. Shi and Z. Chen (e-mail: hyq1304@126.com; czpnchu@163.com).

Abstract: Stimulated Brillouin scattering (SBS) and stimulated Raman scattering (SRS) processes from the aqueous solution of $MgSO_4$ have been observed. The experimental results show that there are three different processes in aqueous solution of sulfate: SBS, SRS attributed to the OH bond stretching vibration of water molecules, and SRS attributed to the stretching vibration of sulfate ion (SO_4^{2-}). The strong and weak sulfate ions determine which one is dominant among the three competition processes. In saturated aqueous solution, it is shown that the SRS process of sulfate ion clearly dominates over the other two stimulated scattering processes. Meanwhile, we have also observed the thermal defocusing phenomenon in saturated aqueous solution at higher pump energy. The results can aid in enhancing the Raman conversion efficiency in liquid scattering media by improving the experimental process.

Index Terms: Stimulated Brillouin scattering (SBS), stimulated Raman scattering (SRS), multiple competition.

1. Introduction

Stimulated scattering in media is an active research topic in non-linear optics. As the third-order nonlinear optical processes, stimulated Brillouin scattering (SBS) and stimulated Raman scattering (SRS) are two kinds of emblematic inelastic scattering processes resulting from the interaction of high-intensity laser with matter [1]–[3]. Over the past few decades, there have been a considerable number of significant theoretical and experimental studies on SBS and SRS, owing to their broad applications, such as pulse compression [4], [5], phase conjugation [6], [7], optical amplification and lasing [8], [9], lidar for remote sensing [10]–[12], optical communication and sensing [13], [14], frequency and wavelength conversion [15], [16], femtosecond and picosecond laser pulses generation [17], [18], and so on.

In terms of the physical mechanisms, SBS is attributed to the interaction of laser beam with acoustic waves, and the SRS process is described as the interaction of laser beam with optical

phonons. The SBS and SRS processes can be obviously enhanced by using the intense laser source. Therefore, when an appropriate intensity laser with sufficient temporal and spatial coherence is employed as the pump laser source, both SBS and SRS can be excited due to the matched energy and momentum conservation conditions. In liquid or high-pressure gas, the competition between SBS and SRS is still the conventional viewpoint [19]–[21]. The first experimental observation of competition between SBS and SRS has been reported by Maier from CS_2 in an optical cell [22]. Since then, the competition between SBS and SRS in gaseous and liquid media has been widely observed from CF_4, CH_4, H_2, water, and alcohol, etc. [23]–[26]. One notable feature in the stimulated scattering process from homogeneous liquid or high-pressure gas is that when a single longitudinal model laser is used as the pump source, the SBS process is clearly strong compared with the SRS process due to the higher Brillouin gain. In this case, the SBS will be dominant since most of the pump laser energy is converted to SBS, and the SRS process will be extremely suppressed. An unconventional physical mechanism could be produced in liquid media (such as water, alcohol) that SRS is pump amplified by backward SBS under the single-model laser pump condition, this pumping effect is benefited from the pulse compression and phase conjugation properties of SBS [27]–[29]. Nonetheless, the intensity of SBS is still higher than the SRS intensity because of the SRS gain is typically two orders of magnitude smaller than the SBS gain. In the process of competition, the SRS may dominate only when the SBS process is greatly restrained. For example, the SBS process can be significantly suppressed by using a wide linewidth laser as the pump source to restrict the Brillouin gain coefficient [30]. The SRS process may dominate also by changing the medium composition to reduce the SBS gain, for example, Jones *et al*. [31] have added helium into methane in their experiment to regulate the SBS gain.

In practical applications, the competition between SBS and SRS goes against the efficient operation of devices based on SBS or SRS process. For instance, the generation of new laser wavelength through frequency conversion by higher-order nonlinear optical process of SRS, the competing SBS process will reduce the frequency conversion efficiency based on SRS. Therefore, it is very significant to figure out the diversiform appearances between SBS and SRS processes in working media.

Our present studies aim to investigate the multiple competition processes between stimulated Brillouin and Raman scattering in a blending sulfate aqueous solution instand of the homogeneous medium, in which the magnesium sulfate ($MgSO_4$) was dissolved into the distilled water with different concentrations. We measured the energies of SBS and SRS from the aqueous solution with different $MgSO_4$ concentrations and analyzed the influence of sulfate ion (SO_4^{2-}) on the SBS and SRS processes. Also, the distribution of the SRS spectra generated from the different medium components was presented. We report the first observation, to our knowledge, of three different competition processes between SBS and SRS from a sulfate aqueous solution.

2. Method and Materials

The schematic diagram of the experimental setup for measuring the SBS and SRS is shown in Fig. 1. A Q-switched Nd: YAG laser (Powerlite Precision Plus, Continuum) operating at 532 nm after through an amplifier and a second harmonic generator (SHG), was used as pump source for exciting SBS and SRS from the medium cell. The pump laser possesses the following parameters: maximum output energy $\sim$700 mJ/Pulse, repetition frequency 10 Hz, pulse duration $\sim$7 ns (full width at half maximum, FWHM), Gaussian spatial profile with $1/e^2$ diameter of 12 mm, divergence angle $\sim$0.45 mrad, and multi-longitudinal mode linewidth $\sim$30 GHz. Fig. 2 shows the temporal profile and the far-field pattern of intensity distribution of the pump laser pulse. The temporal profile was measured by a photodetector (ET-2000, Electro-Optics Technology, Inc.) and an oscilloscope (DSO7104A, Agilent Technologies), and the far-field pattern of the pump laser was measured by using an $f = 90$ cm focusing lens and a CCD-array detector (BC106-VIS, Thorlabs) placed in the focal plane position.

The output beam from the laser source with the vertical polarization was focused into a 1 m long medium cell filled with the $MgSO_4$ aqueous solution by lenses L_1 and L_2 after passing through

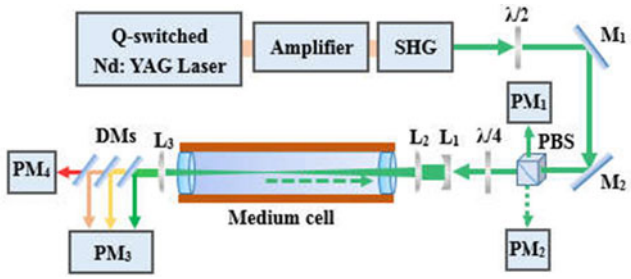

Fig. 1. Schematic diagram of the experimental layout. SHG: second harmonic generator, $\lambda/2$: half-wave plate, $\lambda/4$: quarter-wave plate, PBS: polarization beam splitter, M_1 and M_2: mirrors, L_1-L_3: lenses, PM_1-PM_4: power monitors, DMs: dichroic mirrors.

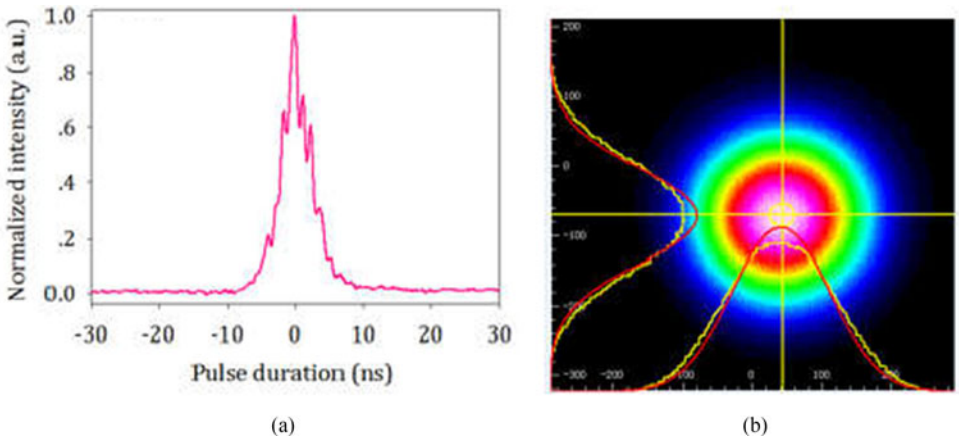

Fig. 2. Measured (a) temporal profile and (b) intensity distribution of the pump laser pulse. Pump energy: ~2 mJ.

$\lambda/2$ plate (horizontal polarization), PBS, and $\lambda/4$ plate (circularly polarization) in turn. The PBS possesses a higher transmittivity (~90%) for horizontal polarization. The SRS and residual pump light coming out of the cell were re-collimated at the exit of the cell window and separated among the different wavelengths by dichroic mirrors (DMs). The dichroic mirrors with >99% reflectivity at 532 nm and >90% of transmittance around Stokes's wavelengths of SRS by coating different films. The signal energy of SBS was measured by PM_2 (818P-001-12, Newport), and the total incident energy was monitored by PM_1 (PM30V1, Coherent). The energy and spectrum of SRS was measured by power monitors (918D-SL-OD3, Newport; PM10V1, Coherent), and a spectrometer with resolution of ~0.4 nm (AvaSpec-ULS2048, Avantes), respectively. The corrections have been made for the energy losses due to the dichroic mirrors and optical windows of medium cell.

The scattering media were prepared by dissolving $MgSO_4$ (analytical-reagent grade, 99% purity) in distilled water of ~23 °C. The content of $MgSO_4$ in saturated aqueous solution was 37 g/100 mL. The prepared original solutions were filtrated by a ~0.5 μm filtrator to filtrate the tiny crystals of $MgSO_4$ and reduce the impurity particles as much as possible. Before the measurement, the filtered solutions were churned up by ultrasonic waves to make the solution uniform.

3. Results and Discussion

According to the pulse duration of pump laser, in order to maintain the effective interaction length for producing the SBS process, the incident pump laser was focused by lenses L_1 and L_2 at the position of 0.9 m in the medium cell. To inspect the influence of sulfate concentration on SBS

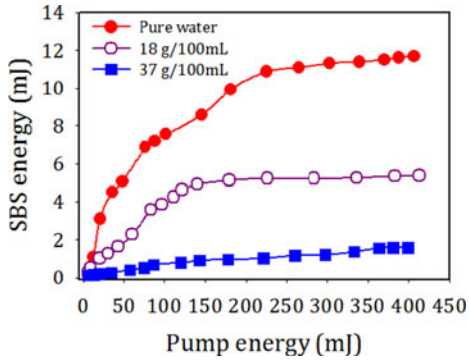

Fig. 3. Measured SBS energy as a function of incident pump energy at different scattering media.

process, we have measured the SBS energy versus the incident pump energy from three different scattering media of pure water, 18 g/100 mL $MgSO_4$ aqueous solution, and 37 g/100 mL $MgSO_4$ saturated aqueous solution, respectively. It is necessary to state that during the process of the whole experiment, the output energy of the pump laser was controlled through changing the different time delay between the amplifier and the oscillator. The measured results of SBS energy are shown in Fig. 3. It can be seen that the SBS energy decreases with the increase of sulfate concentration at the same pump energy. Furthermore, the SBS energy in the same medium concentration increases with the increase of pump energy, but the slope becomes lower gradually when the pump energy is higher than ~150 mJ. The exhibited features from the changes of SBS energy with the pump energy can be explained by the following reasons. (i) The gain coefficient of SBS depends on the viscosity of material, this can be expressed by [32], [33]

$$g_B = \frac{\gamma^2 \omega_s^2 \tau_B}{\rho_0 n c^3 \upsilon_s} \tag{1}$$

$$\tau_B = \frac{\rho_0 c^2}{\eta \omega_s^2 n^2} \tag{2}$$

where γ is the electrostrictive coefficient of the material, ω_s is the frequency of the Stokes component in SBS, ρ_0 and n are the density and the refractive index of the material, respectively, c is the light spend in vacuum, υ_s is the sound speed in the material, τ_B is the phonon lifetime of the material, and η is the viscosity of the material. We can see from the (1) and (2) that the gain coefficient of SBS is inversely proportional to the viscosity of the material. For sulfate aqueous solution, it possesses the higher viscosity than the pure water, resulting in the decrease of the SBS gain so that the SBS process is significantly limited. (ii) Other two competing processes are excited by the intense pump laser pulses that the SRS process attributed to the symmetric stretching vibration of the sulfate ion (SO_4^{2-}), and the SRS process corresponds to the ordinary OH stretching vibration of water molecules. Since the pump source used in this experiment is a multi-longitudinal mode, the forward SRS (FSRS) is dominant and SBS is greatly suppressed by the wide linewidth and the short coherence length [34].

In order to show the relationship between SBS and SRS, we have measured the SRS spectrum from three different scattering media. The evolution of the SRS spectra is shown in Fig. 4, in which all the spectra were normalized by the maximum value at the position of 532 nm. Fig. 4(a) shows the SRS spectrum of distilled water, in which the peak positioned at ~649 nm corresponds to the Stokes Raman scattering component of water. The Stokes Raman shift of water is ~3393 cm^{-1}, which associates with the symmetric OH bond stretching vibration between the water molecules [35], [36]. The anti-Stokes Raman component located at ~436 nm can also be seen due to four-wave mixing (FWM) process. Fig. 4(b) and (c) show the SRS spectra of $MgSO_4$ aqueous solution at two different concentrations. It can be seen that the pump laser wavelength of 532 nm interacting

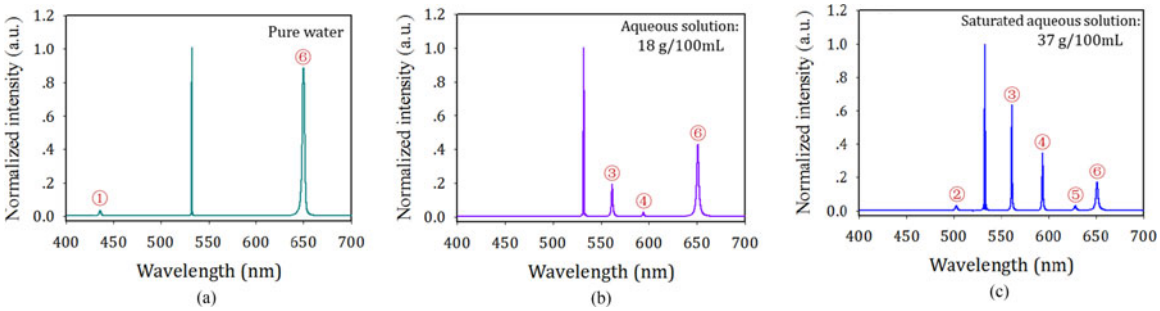

Fig. 4. Measured SRS spectrum distributions from different scattering media at the same pump energy of ~330 mJ. The marked numbers ① and ⑥ represent the anti-Stokes and Stokes peaks of water; ② represents the anti-Stokes peak of sulfate ion; ③– ⑤represents1st, 2nd, and 3rd order Stokes peaks of sulfate ion, respectively.

with the aqueous solution generates the first order Stokes wavelength followed by higher order Stokes peaks. These peaks located at ~561.4, 594, and 630 nm correspond to the 1st, 2nd, and 3rd order Stokes components, respectively, that attributed to the strong symmetric vibrations of tetrahedral structural groups (SO_4^{2-}). The peak located at ~505.4 nm corresponds to the anti-Stokes component of sulfate ion due to the FWM process. Each peak of the 1st and 2nd order Stokes was separated from its neighbor by a Raman shift of ~980 cm^{-1}, which was similar to the spontaneous Raman scattering shift of aqueous solution of $MgSO_4$ observed by A. R. Davis and W. W. Rudolph *et al*. [37], [38], but the Raman shifts of the 3rd order Stokes is about 966 cm^{-1} and smaller than 980 cm^{-1}. We think the concentration dependence of the SO_4^{2-} Raman mode may be the main reason. Another possible factor may be that the component and purity of $MgSO_4$ affect the Raman shift. It can also be noticed from Fig. 4 that with the increase of the $MgSO_4$ concentration, the Stokes peaks of sulfate ion become stronger. In addition, the 1st and 2nd Stokes peaks of sulfate ion present stronger than the Stokes peak of water in saturated aqueous solution, and the additional frequency component of anti-Stokes and 3rd Stokes were excited also. The displayed features from Fig. 4 indicate that the SRS process of sulfate ion is dominant compared with the SRS process of water in saturated aqueous solution. This result is due to the number of laser photons (or the incident laser intensity) and the scattering cross section satisfy the higher gain for producing the SRS process in $MgSO_4$ saturated aqueous solution [2], and meanwhile, the SBS process is greatly suppressed by the higher viscosity of saturated aqueous solution and the short coherence length. That is, the SRS process of sulfate ion is gradually dominant during the stimulated scattering process in aqueous solution with the increase of $MgSO_4$ concentration, and the competing SRS process of water and SBS process are significantly limited.

In order to display more visually the relationship between SBS and SRS processes in aqueous solution, the SRS energies were measured from three different scattering media. The results of this experiment are shown in Fig. 5. It can be seen from Fig. 5(a) that the measured SRS energy of water positioned at 650 nm wavelength decreases with the increase of $MgSO_4$ concentration at the same pump energy, and the slope of the curve decreases at higher contents. This implies that the SRS process attributed to the OH bond stretching vibration of water molecules is efficiently restrained. Fig. 5(b) shows the measured 1st and 2nd order Stokes energies of SRS belong to the stretching vibration of sulfate ion. It can be seen that the energy of 1st order Stokes increases with the increase of pump energy at the same concentration of $MgSO_4$, and also increases with the increase of $MgSO_4$ concentration at the same pump energy. In addition, the measured energy of 2nd Stokes increases with the increase of pump energy in the saturated aqueous solution of 37 g/100 mL $MgSO_4$, as shown in the right ordinate of Fig. 5(b). Since the 2nd Stokes energy of sulfate ion in the 18 g/100 mL aqueous solution is too weak to measure by using our present experimental conditions, we did not give the result in this paper. We can conclude from Fig. 5 that the SRS process of sulfate ion is much more efficient than the SRS process of water in saturated

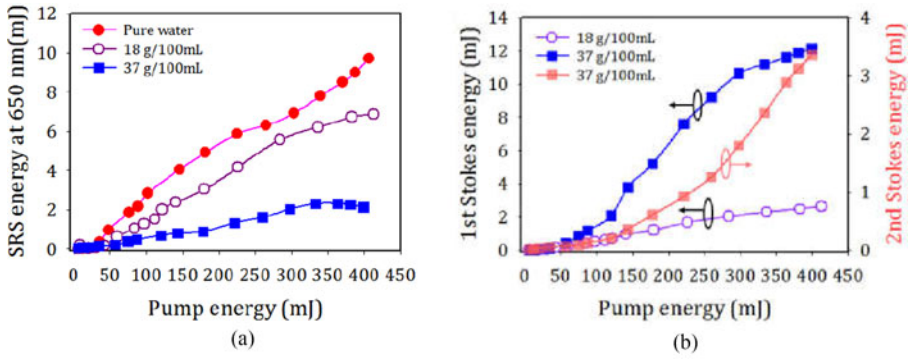

Fig. 5. Measured SRS energies of (a) Stokes at 650 nm belongs to water and (b) 1st and 2nd order Stokes belong to sulfate ion (SO_4^{2-}).

aqueous solution. That is, the SRS process of sulfate ion is dominant compared with the other two stimulated scattering processes in saturated aqueous solution at the same pump conditions.

To the nonlinear stimulated scattering process in liquid media, an important factor must be taken into account that the refractive index–temperature derivatives dn/dT. The refractive index and its derivatives with respect to temperature is an important optical properties of liquid mixtures and has come to play an important role. One of the most common physical performances is the thermal distortion of high power laser beams traversing optical media. Under most conditions, the associated optical thermal distortion is approximately proportional to dn/dT [39], [40]. When a pump laser beam with a Gaussian intensity distribution is incident upon the scattering medium, the dependence of the refractive index on the light intensity can be expressed by [41]

$$n = n_0 + n_2 I \tag{3}$$

where n_0 is the unperturbed refractive index, n_2 is the nonlinear refractive index coefficient, and I is the light intensity of pump laser. For nonlinear stimulated scattering process, for example, SRS process in sulfate aqueous solution, each Stokes shifted photon loses $\sim$980 cm^{-1} of energy to the sulfate ion vibrational mode. The lost energies will be absorbed by the scattering medium, resulting in a change in the nonlinear refractive index. In this case, the refractive index decreases with an increasing temperature, that is, existing a negative derivative of the refractive index, $n_2 < 0$. It can be expressed by a first-order approximation

$$n = n_0 + \frac{dn}{dT}T, \ \frac{dn}{dT} < 0. \tag{4}$$

Consequently, the decrease in refractive index with temperature leads in a stationary scattering medium to a thermal defocusing.

In this paper, we have observed the thermal defocusing by measuring the intensity distribution of the residual pump laser beam as a function of pump energy at the exit of the cell window. Fig. 6 shows the measured far-field patterns of intensity distribution of the residual pump beam from saturated aqueous solution by using the CCD-array detector placed at the exit of the cell window after through a certain attenuation. The pixel size of CCD-array is 6.5 μm in square. Each of the images shown in Fig. 6 was captured after three hundred pump pulses enter the medium cell with three different pump energy of 50, 100, and 300 mJ/Pulse, respectively. It can be seen from the far-field images that the intensity distribution of the residual pump beam presents an intensity irregularity with the increase of pump energy. Furthermore, it is clear that the effective beam diameter increases from 237 pixels to 398 pixels with the increase of pump energy. That is, large pump pulse energies lead to an obvious thermal defocusing or so-called “thermal blooming” effect, as shown in Fig. 6(c).

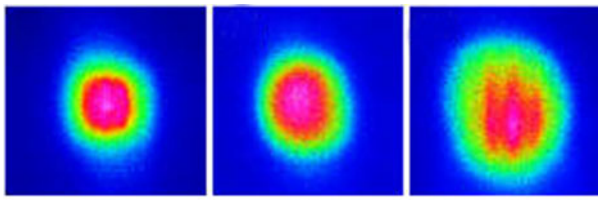

Fig. 6. Far-field images of intensity distribution of the pump beam at the exit of the cell window for different pump energy of (a) ∼50 mJ/Pulse, (b) ∼100 mJ/Pulse, and (c) ∼300 mJ/Pulse. The effective beam diameter is 237, 291, and 398 pixels, respectively.

The thermal defocusing effect can degenerate the beam quality inside the Raman cell, increase the waist radius, and change the optical properties of scattering media, resulting in the reduction of the conversion efficiency of stimulated scattering process. Nevertheless, the thermal defocusing effect could be minimized by cooling the liquid media to near the freezing temperature, namely, $dn/dT = 0$. The more specific investigation on the efficient wavelength conversion based on SRS and the refractive index-temperature change in a blending aqueous solution system will be the subject of further studies.

4. Conclusion

In conclusion, we have conducted an experimental study of SBS and SRS processes in $MgSO_4$ aqueous solution pumped by 532 nm laser pulses. The experimental results show that there are three different stimulated scattering processes in aqueous solution system, they are SBS, SRS belongs to sulfate ion, and SRS belongs to water. In saturated aqueous solution of $MgSO_4$, the SRS process attributed to the stretching vibration of sulfate ion is the dominant process compared with the two other processes. Meanwhile, the 1st (561.4 nm), 2nd (594 nm), and 3rd (630 nm) order Stokes spectroscopies of sulfate ion were observed, indicating that the saturated aqueous solution of sulfate can be potentially used to generate the new laser wavelengths through SRS process. Also, the thermal defocusing phenomenon in saturated aqueous solution at higher pump energy has been observed, it goes against the conversion efficiency of stimulated scattering process.

References

[1] Y. R. Shen and N. Bloembeagen, "Theory of stimulated Brillouin and Raman scattering," *Phys. Rev.*, vol. 137, no. 6A, pp. 1787–1805, 1965.
[2] R.W. Boyd, *Nonlinear Optics*. San Diego, CA, USA: Academic, 1992.
[3] M. J. Damzen, V. I. Vlad, V. Babin, and A. Mocofanescu, *Stimulated Brillouin Scattering: Fundamentals and Applications*. Boca Raton, FL, USA: CRC Press, 2003.
[4] D. T. Hon, "Pulse compression by stimulated Brillouin scattering," *Opt. Lett.*, vol. 5, no. 12, pp. 516–518, 1980.
[5] D. Neshev, I. Velchev, W. A. Majewski, W. Hogervorst, and W. Ubachs, "SBS pulse compression to 200 ps in a compact single-cell setup," *Appl. Phys. B*, vol. 68, no. 4, pp. 671–675, 1999.
[6] B. Králiková, J. P. Skála Straka, and H. Turčičová, "High-quality phase conjugation even in a highly transient regime of stimulated Brillouin scattering," *Appl. Phys. Lett.*, vol. 77, no. 5, pp. 627–629, 2000.
[7] A. Kuzmin, E. Khazanov, O. Kulagin, and A. Shaykin, "Neodymium glass laser with a phase conjugate mirror producing 220 J pulses at 0.02 Hz repetition rate," *Opt. Exp.*, vol. 22, no. 17, pp. 20842–20855, 2014.
[8] Z. Lu, W. Gao, W. He, Z. Zhang, and W. Hasi, "High amplification and low noise achieved by a double-stage non-collinear Brillouin amplifier," *Opt. Exp.*, vol. 17, no. 13, pp. 10675–10680, 2009.
[9] Q. Guo, Z. Lu, and Y. Wang, "Highly efficient Brillouin amplification of strong Stokes seed," *Appl. Phys. Lett.*, vol. 96, no. 22, 2010, Art. no. 221107.
[10] J. Shi *et al.*, "A lidar system based on stimulated Brillouin scattering," *Appl. Phys. B*, vol. 86, no. 1, pp. 177–179, 2007.
[11] J. Shi, M. Ouyang, W. Gong, S. Li, and D. Liu, "A Brillouin lidar system using F–P etalon and ICCD for remote sensing of the ocean," *Appl. Phys. B*, vol. 90, no. 3, pp. 569–571, 2008.
[12] B. Zhou *et al.*, "Experimental analysis on the rapid measurement of a high precision Brillouin scattering spectrum in water using a Fabry–Pérot etalon," *Laser Phys. Lett.*, vol. 13, no. 5, 2016, Art. no. 055701.

[13] K. D. Park, B. Min, P. Kim, N. Park, J. H. Lee, and J. S. Chang, "Dynamics of cascaded Brillouin–Rayleigh scattering in a distributed fiber Raman amplifier," *Opt. Lett.*, vol. 27, no. 3, pp. 155–157, 2002.
[14] T. Kurashima, T. Horiguchi, and M. Tateda, "Distributed-temperature sensing using stimulated Brillouin scattering in optical silica fibers," *Opt. Lett.*, vol. 15, no. 8, pp. 1038–1040, 1990.
[15] Y. Ganot and I. Bar, "Efficient frequency conversion by stimulated Raman scattering in a sodium nitrate aqueous solution," *Appl. Phys. Lett.*, vol. 107, no. 13, 2015, Art. no. 131108.
[16] V. Pasiskevicius, A. Fragemann, F. Laurell, R. Butkus, V. Smilgevicius, and A. Piskarskas, "Enhanced stimulated Raman scattering in optical parametric oscillators from periodically poled KTiOPO," *Appl. Phys. Lett.*, vol. 82, no. 3, pp. 325–327, 2003.
[17] V. Kalosha, M. Spanner, J. Herrmann, and M. Ivanov, "Generation of single dispersion precompensated 1-fs pulses by shaped-pulse optimized high-order stimulated Raman scattering," *Phys. Rev. Lett.*, vol. 88, no. 10, 2002, Art. no. 103901.
[18] J. Findeisen, H. J. Eichler, and A. A. Kaminskii, "Efficient picosecond PbWO4 and two-wavelength KGd (WO4)2 Raman lasers in the IR and visible," *IEEE J. Quantum Electron.*, vol. 35, no. 2, pp. 173–178, Feb. 1999.
[19] C. J. Walsh, D. M. Villeneuve, and H. A. Baldis, "Electron plasma-wave production by stimulated Raman scattering: Competition with stimulated Brillouin scattering," *Phys. Rev. Lett.*, vol. 3, no. 15, pp. 1445–1448, 1984.
[20] X. Hu, W. Chen, M. Chen, and Z. Meng, "Experimental observation of the competition between stimulated Brillouin scattering, modulation instability and stimulated Raman scattering in long single mode fiber," *J. Opt.*, vol. 8, no. 8, 2016, Art. no. 085501.
[21] K. Estabrook and W. L. Kruer, "Nonlinear features of stimulated Brillouin and Raman scattering," *Phys. Fluids B*, vol. 1, no. 6, pp. 1282–1286, 1989.
[22] M. Maier, W. Kaiser, and J. A. Giordmaine, "Intense light bursts in the stimulated Raman effect," *Phys. Rev. Lett.*, vol. 17, no. 26, pp. 1275–1277, 1966.
[23] B. Snow, S. X. Qian, and R. K.Chang, "Stimulated Raman scattering from individual water and ethanol droplets at morphology-dependent resonances," *Opt. Lett.*, vol. 10, no. 1, pp. 37–39, 1985.
[24] L. B. Yehud, D. Belker, G. Ravnitzki, and A. A. Ishaaya, "Competition between stimulated Raman and Brillouin scattering processes in CF4 gas," *Opt. Lett.*, vol. 39, no. 4, pp. 1026–1029, 2014.
[25] K. Sentrayan and V. Kushawaha, "Competition between steady state stimulated Raman and Brillouin scattering processes in CH4 and H2," *J. Phys. D*, vol. 26, no. 10, pp. 1554–1560, 1993.
[26] J. Shi, W. Chen, X. Mo, J. Liu, X. He, and K. Yang, "Experimental investigation on the competition between wideband stimulated Brillouin scattering and forward stimulated Raman scattering in water," *Opt. Lett.*, vol. 37, no. 14, pp. 2988–2990, 2012.
[27] J. Shi *et al.*, "Stimulated Raman scattering enhanced by stimulated Brillouin scattering," *Opt. Lett.*, vol. 34, no. 7, pp. 977–979, 2009.
[28] J. Shi *et al.*, "Unconventional physical mechanisms between stimulated Brillouin scattering and backward stimulated Raman scattering in liquid water," *J. Opt.*, vol. 13, no. 7, 2011, Art. no. 075201.
[29] J. Z. Zhang, G. Chen, and R. K. Chang, "Pumping of stimulated Raman scattering by stimulated Brillouin scattering within a single liquid droplet: Input laser linewidth effects," *J. Opt. Soc. Amer. B*, vol. 7, no. 1, pp. 108–115, 1990.
[30] G. C. Valley, "A review of stimulated Brillouin scattering excited with a broad-band pump laser," *IEEE J. Quantum Electron.*, vol. 22, no. 5, pp. 704–712, May 1986.
[31] D. C. Jones, M. S. Mangir, D. A. Rockwell, and J. O. White, "Stimulated Brillouin scattering gain variation and transient effects in a CH4: He binary gas mixture," *J. Opt. Soc. Amer. B*, vol. 7, no. 10, pp. 2090–2096, 1990.
[32] R.W. Boyd and K. Rzazewski, "Noise initiation of stimulated Brillouin scattering," *Phys. Rev. A*, vol. 42, no. 9, pp. 5514–5521, 1990.
[33] J. Shi *et al.*, "Temperature dependence of threshold and gain coefficient of stimulated Brillouin scattering in water," *Appl. Phys. B*, vol. 108, no. 4, pp. 717–720, 2012.
[34] J. Shi, X. Chen, M. Ouyang, J. Liu, and D. Liu, "Theoretical investigation on the threshold value of stimulated Brillouin scattering in terms of laser intensity," *Appl. Phys. B*, vol. 95, no. 4, pp. 657–660, 2009.
[35] B. M. Auer and J. L. Skinner, "IR and Raman spectra of liquid water: Theory and interpretation," *J. Phys. Chem.*, vol. 128, no. 22, 2008, Art. no. 224511.
[36] T. Li *et al.*, "Influence of strong and weak hydrogen bonds in ices on stimulated Raman scattering," *Opt. Lett.*, vol. 41, no. 6, pp. 1297–1300, 2016.
[37] A. R. Davis and B. G. Oliver, "Raman spectroscopic evidence for contact ion pairing in aqueous magnesium sulfate solutions," *J. Phys. Chem.*, vol. 77, no. 10, pp. 1315–1316, 1973.
[38] W. W. Rudolph, G. Irmerb, and G. T. Hefter, "Raman spectroscopic investigation of speciation in MgSO4(aq)," *Phys. Chem. Chem. Phys.*, vol. 5, pp. 5253–5261, 2003.
[39] Y. Tsay, B. Bendow, and S. S. Mitra, "Theory of the temperature derivative of the refractive index in transparent crystals," *Phys. Rev. B*, vol. 8, no. 6, pp. 2688–2696, 1973.
[40] G. Abbate, U. Bernini, E. Ragozzino, and F. Somma, "The temperature dependence of the refractive index of water," *J. Phys. D: Appl. Phys.*, vol. 11, no. 8, pp. 1167–1172, 1978.
[41] B. Richerzhagen, G. Delacrétaz, and R. P. Salathe, "Complete mode1978; I to simulate the thermal defocusing of a laser beam focused in water," *Opt. Eng.*, vol. 35, no. 7, pp. 2058–2066, 1996.